Asia-Pacific J. Atmos. Sci., 46(3), 341-353, 2010
DOI:10.1007/s13143-010-1003-2

High-Resolution Summer Rainfall Prediction in the JHWC Real-Time WRF System

Dong-Kyou Lee, Dae-Yong Eom, Joo-Wan Kim and Jae-Bok Lee

Atmospheric Sciences Program, School of Earth and Environmental Sciences, Seoul National University, Seoul, Korea

(Manuscript received 8 Jan 2010; revised 22 March 2010, accepted 28 April 2010)

Abstract: The WRF-based real-time forecast system (http://jhwc.snu.ac.kr/weather) of the Joint Center for High-impact Weather and Climate Research (JHWC) has been in operation since November 2006; this system has three nested model domains using GFS (Global Forecast System) data for its initial and boundary conditions. In this study, we evaluate the improvement in daily and hourly weather prediction, particularly the prediction of summer rainfall over the Korean Peninsula, in the JHWC WRF (Weather Research and Forecasting) model system by 3DVAR (three-Dimensional Variational) data assimilation using the data obtained from KEOP (Korea Enhanced Observation Program). KEOP was conducted during the period June 15 to July 15, 2007, and the data obtained included GTS (Global Telecommunication System) upper-air sounding, AWS (Automatic Weather System), wind profiler, and radar observation data. Rainfall prediction and its characteristics should be verified by using the precipitation observation and the difference field of each experiment. High-resolution (3 km in domain 3) summer rainfall prediction over the Korean peninsula is substantially influenced by improved synoptic-scale prediction in domains 1 (27 km) and 2 (9 km), in particular by data assimilation using the sounding and wind profiler data. The rainfall prediction in domain 3 was further improved by radar and AWS data assimilation in domain 3. The equitable threat score and bias score of the rainfall predicted in domain 3 indicated improvement for the threshold values of 0.1, 1, and 2.5 mm with data assimilation. For cases of occurrence of heavy rainfall (7 days), the equitable threat score and bias score improved considerably at all threshold values as compared to the entire period of KEOP. Radar and AWS data assimilation improved the temporal and spatial distributions of diurnal rainfall over southern Korea, and AWS data assimilation increased the predicted rainfall amount by approximately 0.3 mm $3hr^{-1}$.

Key words: WRF-3DVAR, WRF model real-time operation, KEOP, summer rainfall prediction, diurnal variation of rainfall

1. Introduction

Mesoscale numerical weather prediction by using mesoscale models (the Fifth-Generation Mesoscale Model (MM5), Grell *et al.,* 1994; Weather Research and Forecasting (WRF) model, Skamarock *et al.,* 2005) has played an important role in operational as well as severe weather forecasting by high-performance computing. High-resolution mesoscale models can contribute to localized weather forecasting, particularly in areas where the topography and land-use heterogeneity modulate synoptic-scale weather. Furthermore, the validational studies of these mesoscale models, which is essential in terms of model predictability, has been gaining interest in the recent years.

The Joint Center for High-impact Weather and Climate Research real-time Numerical Weather Prediction (NWP) system is based on the WRF model and has been in daily operation over the East Asia domain using GFS data from November 2006. The system is run on a Linux cluster machine at the National Supercomputer Center of the Korea Institute of Science and Technology Information (KISTI), and the model output data have been archived. The WRF model has been carefully evaluated on a test-bed facility to obtain its performance and error statistics over the Korean Peninsula as well as East Asia in order to understand high-impact weather and improve its predictability (Lee *et al.,* 2008a).

Nonconventional observation such as meteorological satellites and radars provide additional and sufficient information for mesoscale data assimilation. Variational assimilation (e.g., 3DVAR, 4DVAR) has become a predominant method for providing initial model data. However, variational assimilation techniques are yet to be successfully applied for severe weather forecasting, especially the amount of heavy rainfall, in Korea and East Asia. Therefore, it is imperative to conduct mesoscale model tests and verify the results to provide a direction for the improvement of model forecasts. Quantitative precipitation forecasting (QPF) using mesoscale models for severe weather has been one of the most challenging problems in operational numerical weather prediction.

A number of studies have verified the predictability of mesoscale model using either routine meteorological observations or data obtained from intensive field experiments. Many of these studies such as those by Chen *et al.* (2002), and Colle *et al.* (2003a, b) have focused on QPF and evaluated various statistical techniques because high resolution mesoscale models offer great potential for improved QPF. Summer rainfall, including heavy rainfall, in Korea frequently occurs over the monsoon front (Changma in Korea), which is influenced by mid-latitude disturbances and directly and indirectly associated with typhoons (Lee *et al.*, 1991, 1998, 2008b). The intensive severe weather responsible for heavy rainfall often develops along the Changma front in Korea (Kim and Lee, 2006). In particular, heavy rainfall is usually the result of individual

Corresponding Author: Prof. Dong-Kyou Lee, Atmospheric Sciences Program, School of Earth and Environmental Sciences, Seoul National University, 599 Gwanak-ro, Gwanak-gu, Seoul 151-747, Korea.
E-mail: dklee@snu.ac.kr

mesoscale storms or mesoscale convective systems (MCSs) embedded in synoptic-scale disturbances.

In order to understand and improve the predictability of complex weather phenomena such as heavy rainfall, it is necessary to obtain observation data with high temporal and spatial resolutions (Langland *et al.*, 1999). Observation experiments that were carried out to understand the importance of intensive observation include TAMEX (Taiwan Area Mesoscale Experiment; Kuo and Chen, 1990), FASTEX (Front and Atlantic Storm-Track Experiment; Joly *et al.*, 1999), IHOP (International H2O project; Tammy *et al.*, 2004), and SoWMEX/TiMREX (Southwest Monsoon Experiment/Terrain influenced Monsoon Rainfall Experiment; Lee and Jou, 2008). The scientific objectives of these field experiments were to investigate the physical processes associated with heavy-rain-producing MCSs and estimate the QPE/QPF capabilities of the numerical models. The ultimate goal of these programs is to improve the ability to forecast heavy-rain-producing convective systems, and the associated QPE/QPF. The KEOP (Korea Enhanced Observing Program; Kim and Park, 2008) was launched in 2001 to improve the analysis/forecast of high-impact weather systems, and has primarily been used during the Changma season. In addition, KOEP provides an integrated observational data set to evaluate the forecast impacts of data assimilation systems and the performance of mesoscale models.

In this paper, the ongoing work at the JHWC for the verification and evaluation of the WRF-ARW and the WRF data assimilation system (WRF-3DVAR) using the KEOP-2007 data is documented. In Section 2, the characteristics of the 2007 Changma season are described. In Section 3, data assimilation using the KEOP data is explained. In Section 4, the results of WRF-3DVAR and WRF-ARW are presented. In section 5, a summary and discussion of the results is provided.

2. Observational Results of the KEOP-2007

The KEOP-2007 project was conducted from June 15 to July 15, 2007, in order to analyze and understand the Changma front and high-impact weather systems. Figure 1 shows a time-longitude diagram of the averaged sea-level-pressure and 850 hPa relative vorticity in the 32-35°N latitudinal band, where the monsoon rain band was located, along with the 3 h accumulated rainfall time series of station-averaged and area-averaged (34-39°N, 120-125°E) TRMM (Tropical Rainfall Measuring Mission) data over Korea during the one-month period. During this period, the rainfall events over the southern Korean Peninsula are directly associated with synoptic-scale disturbances. Before approximately June 21, the subtropical high dominated over the southern Korean Peninsula due to which rainfall did not occur. From June 21 to July 16, low-pressure systems frequently propagate eastward along the monsoon rain band over the Korean Peninsula. Although relative vorticity develops at 850 hPa over the southern Korean Peninsula, it apparently does not cause heavy rainfall. In this study, a heavy rainfall case is defined

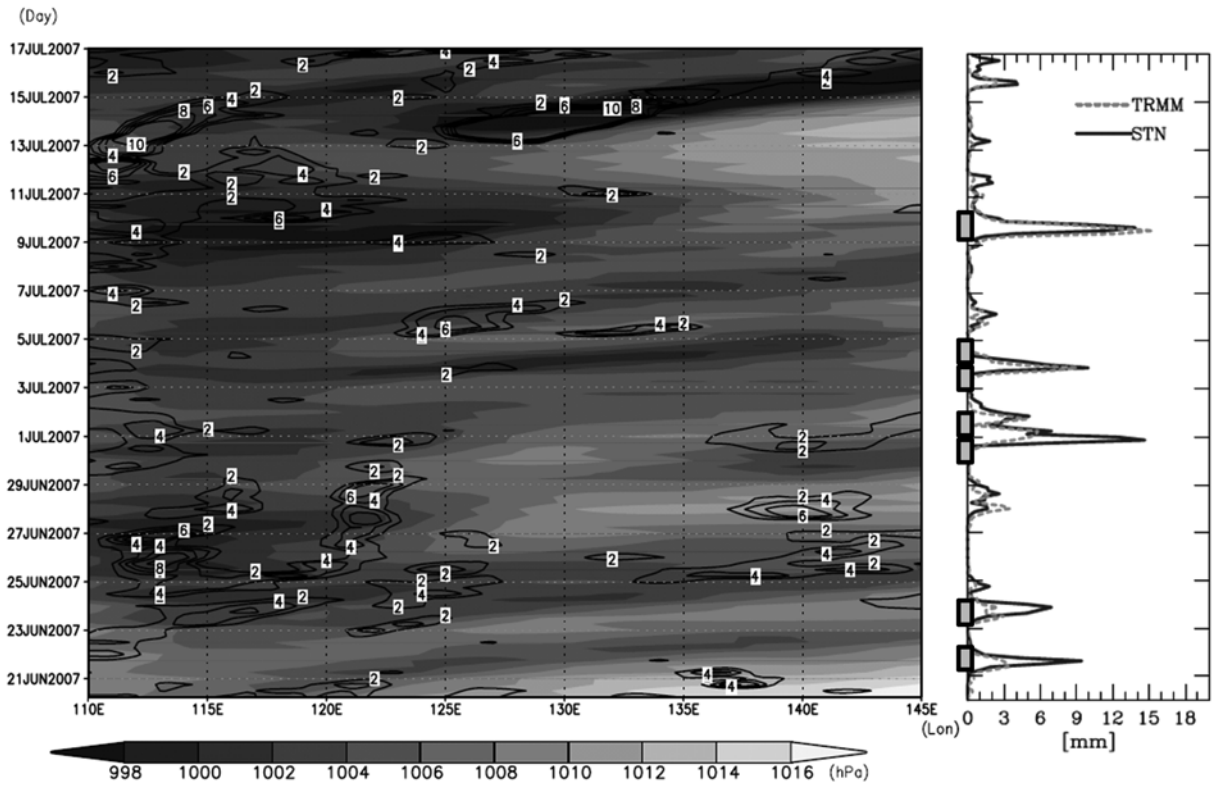

Fig. 1. Time-longitude (Hovmueller) diagram of averaged sea-level-pressure and 850 hPa relative vorticity on the 32-35°N latitudinal band where the monsoon rain band was located (left), and the 3 h accumulated rainfall time series of station-averaged and area-averaged (34-39°N, 120-125°E) TRMM over Korea (right) during the one-month period.

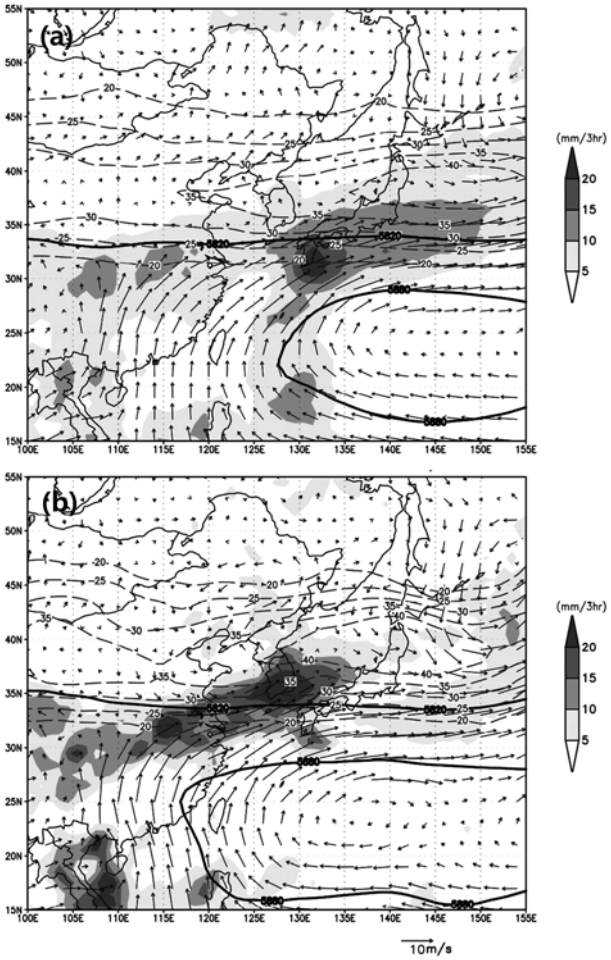

Fig. 2. Time-averaged synoptic patterns during (a) the entire and (b) the heavy rainfall cases: upper-level wind (dashed), 500 hPa geopotential height (solid), low level wind vector (arrow) using FNL, and GPCP rainfall distribution (shaded).

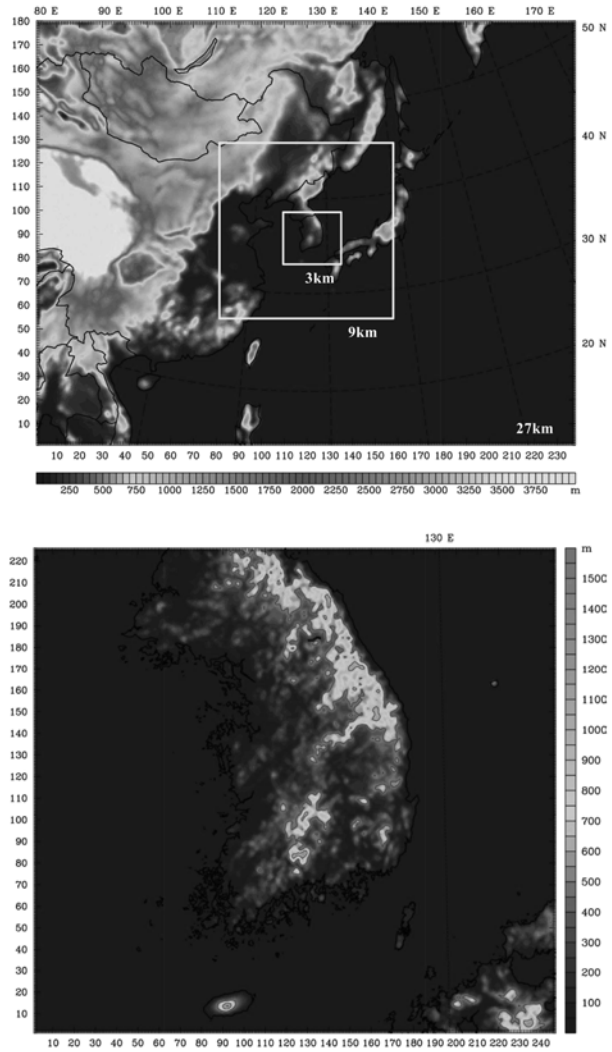

Fig. 3. Model domains: 27 km, 9 km, and 3 km with terrain heights.

by a daily amount of rain greater than 80 mm. We consider two rainfall periods: the entire period of KEOP and the averaged period of five heavy rainfall cases.

The time-averaged synoptic-scale patterns analyzed using the FNL (Final) analysis and GPCP (Global Precipitation Climatology Project) data are shown in Fig. 2. The heavy rainfall case is characterized by an intensified and further westward extended subtropical high, intensified low-level southerly and westerly jet, active northerly flows east of northern Japan, and intensified upper-level westerly jet; these conditions are favorable for heavy rainfall. The rainfall occurs mainly over southern Japan for the entire period while heavy rainfall occurs mainly over central China, southern Yellow Sea, and southern Korea. According to previous studies (Sun and Lee, 2002; Lee *et al*., 2008b), favorable conditions for heavy rainfall in Korea are characterized by warm advection with a southwesterly low-level jet (LLJ), cold-air advection associated with upper-level disturbances, a warm moisture tongue originating from southern or central China, an intensified upper-level jet (ULJ) with strong baroclinicity, and potential instability due to sufficient moisture.

3. Data Assimilation and Model Experiments

Figure 3 shows the model domains. The ARW model (version 2.2)/WRF is run for 72 h forecast in domain 1, 48 h forecast in domain 2, and 24 h forecast in domain 3 with one-way nested grids. The NCEP GFS (Global Forecast System) 0.5° resolution data are used for the boundary and initial conditions. The horizontal resolutions are 27 km in domain 1, 9 km in domain 2, and 3 km in domain 3, which mainly cover East Asia, the Korean Peninsula and the ocean near the peninsula, and South Korea, respectively. The vertical layer in each domain consists of 35 vertical layers, with the model top corresponding to 50 hPa. Table 1 shows the simulation setup for this study.

WRF-3DVAR has been fully developed for the Advanced Research WRF (ARW) model (Barker *et al.*, 2003, 2004). The WRF 3DVAR background error covariance is estimated using the National Meteorological Center (NMC) method (Parrish and Derber, 1992). The incremental cost function is minimized by the conjugate gradient method. The Rapid Update Cycle (RUC) technique is an analysis/forecast cycling technique used in

Table 1. Simulation setup.

Description	Domain 1	Domain 2	Domain 3
Horizontal Grid Size (km)	27	9	3
Horizontal Grid Num.	238 × 180	238 × 226	247 × 226
Vertical Layers / Top	35 eta layers / 50 hPa		
Time Interval (sec.)	120	50	18
Explicit Moisture	WSM 6-class		
Cumulus Parameterization	Kain-Fritsh		None
Boundary Layer	YSU		
Long-wave Radiation	RRTM radiation		
Short-wave Radiation	Dudhia		
Surface physics	Noah land-surface model		

3DVAR data assimilation. RUC as an operational numerical prediction technique for North America continues to be the hourly update assimilation and mesoscale forecast cycling technique used on the isentropic-sigma hybrid vertical coordinates (Benjamin *et al.*, 2004a, b). RUC for high-frequency mesoscale analysis and forecast model systems is widely used as a guide for short-range weather forecasting, particularly by severe weather, aviation, and situational awareness forecasters. In this study, RUC for domains 1, 2, and 3 was carried out at intervals of 6 h (RUC_6hr), 1 h (RUC_1hr), and 30 min (RUC_30min), respectively. Figure 4 shows the assimilation experiments using RUC initialization and the forecast period in each domain.

The KEOP-2007 consisted of an observation network with 6 operational and 4 additional upper-air sounding locations, and 615 operational automatic weather station (AWS), 5 wind profilers, and 10 Doppler radar sites on the southern Korean Peninsula during the KEOP period. In this study, we added the data obtained from 50 AWS and 5 radar sites of the ROKAF (Republic Of Korea Air Force) to the KEOP data. Table 2 and Figure 5 show the descriptions and networks of observation which is used in data assimilation for this study. In particular, the wind and reflectivity fields for the radar assimilation experiments over the Korean Peninsula were extracted from the NCAR Sorted Position Radar INTerpolation (SPRINT) and Custom Editing and Display of Reduced Information in Cartesian Space (CEDRIC) packages (Park and Lee, 2009).

In this study, we conducted ten data assimilation experiments

Table 2. Description of KEOP-2007 data.

Observation type	Number of stations	Used variables for data assimilation	Data interval
Sonde	10	H, T, U, V, Td	6 hours
AWS	685	P, T, U, V, RH	1 hour
Wind Profiler	5	U, V	10 minutes
radar	15	Radial velocity, reflectivity	10 minutes

for model-initial data and forecast experiments, and investigated the performance of QPF by using the results of the JHWC real-time system with and without the assimilation of the KEOP data during a 26-day period (from June 20 to July 15) during the 2007 Changma season. Table 3 lists a summary of the data assimilation and model experiments in all domains in this study. For data assimilation, we considered upper-air sounding, wind profiler, AWS, and radar data to investigate the impact of the data sets on summer rainfall forecasts. In particular, we used the GTS (Global Telecommunication System) data in domain 1; upper-air sounding, wind profiler, and AWS data in domain 2; and AWS and radar data in domain 3. The results for domains 1 and 2 were used to focus on the environmental conditions and their rainfall patterns, while the QPF and forecast characteristics of heavy rainfall were examined from the results for domain 3.

The experimental results were validated using three approaches. The horizontal and vertical distributions of the bias of forecast variables were estimated in domains 1 and 2 against the FNL and radiosonde data, and the vertical bias of the wind was estimated against the wind profiler data. The statistical scores of the equitable threat score (ETS) and bias score (BS) were evaluated for three rainfall threshold values (0.1, 1, and 2.5 mm) using the hourly rainfall forecasts in domains 2 and 3 (Jollie and Stephenson, 2003). Finally, the diurnal cycle and distribution of the forecast rainfall over the southern Korean Peninsula were investigated. The diurnal variation in rainfall is one of the most difficult problems in model forecasting (Davis *et al.*, 2003; Clark *et al.*, 2007).

4. Results of Experiments

Many works (Anthes *et al.*, 1985; Weisman and Klemp, 1986;

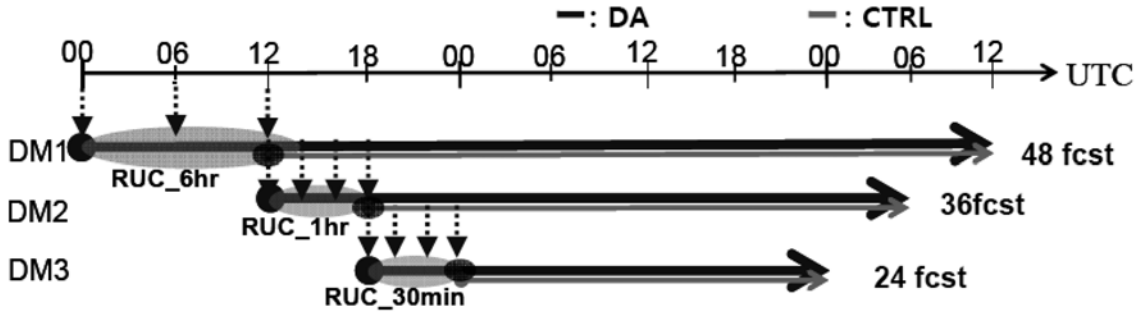

Fig. 4. Assimilation experiment using the RUC initialization and forecast periods.

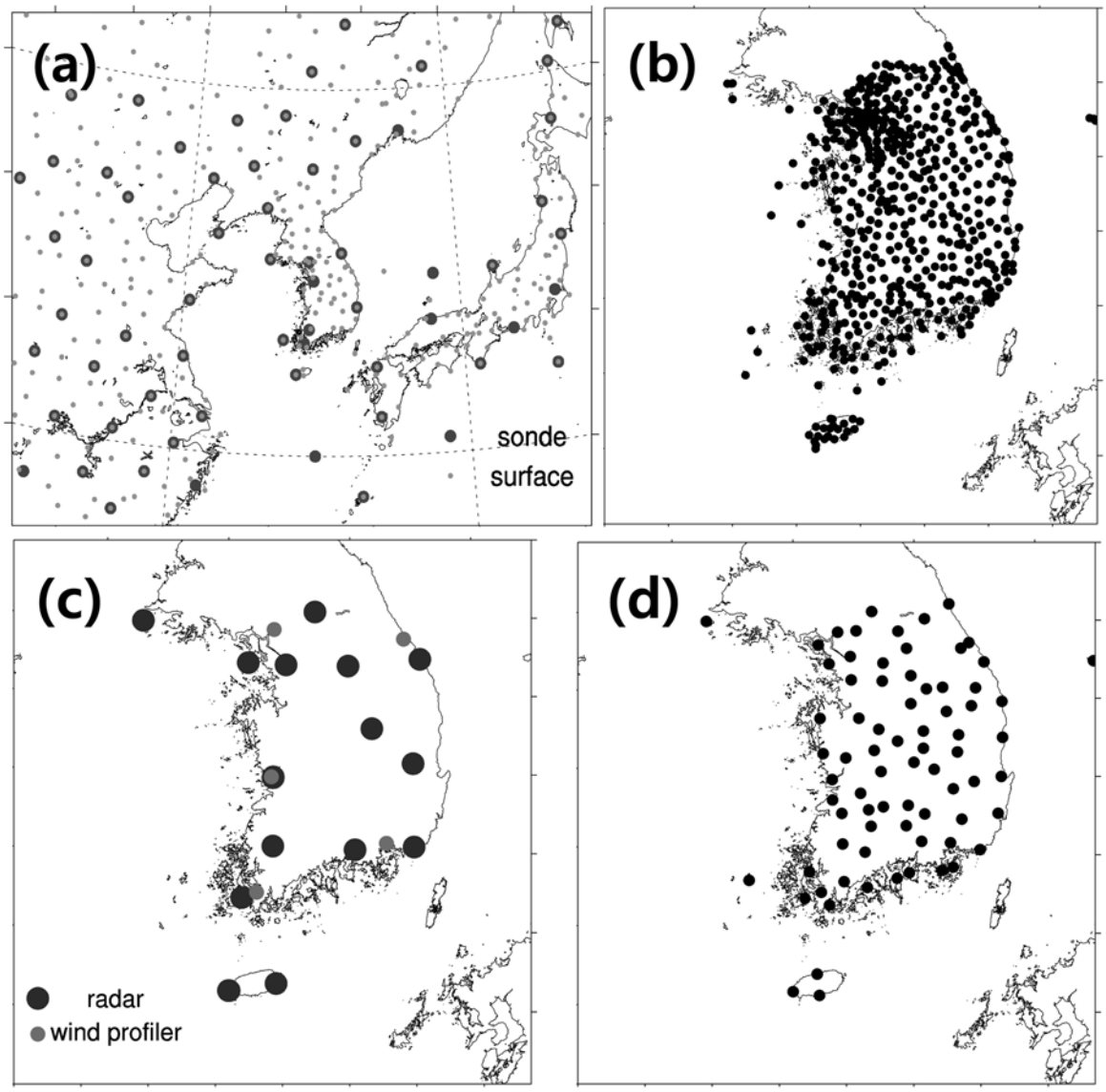

Fig. 5. Networks of observations: (a) Surface and sounding, (b) AWS, (c) radar and wind profiler, and (d) KMA weather stations for the KEOP-2007 over the Korean Peninsula.

Table 3. Summary of data and assimilation setup in all domains.

Experiment	Data and assimilation setup
CTRLD1	JHWC RTF
EXP1D1	GTS assimilation with RUC_6 hr
CTRLD2	JHWC RTF
EXP1D2	Nested in EXP1D1, and no assimilation in DM2
EXP2D2	Nested in EXP1D1, and GTS upper-air and wind profiler assimilation with RUC_1 hr in DM2
EXP3D2	Nested in EXP1D1, and GTS, wind profiler, and AWS assimilation with RUC_1 hr in DM2
CTL3D3	JHWC RTF
EXP1D3	Nested in EXP2D2, and no assimilation in DM3
EXP2D3	Nested in EXP2D2, and RADAR assimilation with RUC_30 min in DM3
EXP3D3	Nested in EXP2D2, and RADAR assimilation with RUC_30 min and AWS assimilation with RUC_1 hr in DM3

Warner *et al.*, 1997; Weisman and Trapp, 2003) suggested that accurate large-scale forcing as lateral boundary conditions can significantly reduce error growth for high-resolution limited-area models which use large-scale forcing, since the large-scale information constantly sweeps through the inflow boundaries. Data assimilation using GTS data, which can improve the forecast in domain 1, is a necessary process to improve the predictability in the nested domains (2 and 3) by providing a better synoptic-scale environment and forcing. Figure 6 shows the vertical distribution of the mixing ratio and temperature biases between the radiosonde data and the experiments for the 12 f (12 h forecast) to 36 f (36 h forecast) forecasts per 6 h interval in domain 1. Unlike CTRLD1, EXP1D1 reduces the bias of the mixing ratio in the low and middle levels (from 850 to 400 hPa). However, the differences between CTRLD1 and EXP1D1 at 18 f and 30 f are small. The 18 f and 30 f are the times at which larger rainfall amounts occur compared to the other times in South Korea. This implies that the data assimilation in domain 1 is little sensitive for the moisture field during the rainfall period. The improvement in the temperature bias in EXP1D1 seems to depend on the forecast time and vertical level. EXP1D1 tends to reduce the negative temperature bias at the low levels and the positive bias at the upper levels compared to CTRLD1. The seasonal verification of the JHWC real-time forecast system showed a negative bias at the low levels and a positive bias at the upper levels in East Asia (Lee *et al.*, 2008a). With the data assimilation using the GTS data, EXP1D1 reduced the model systematic bias slightly at the forecast times. Overall,

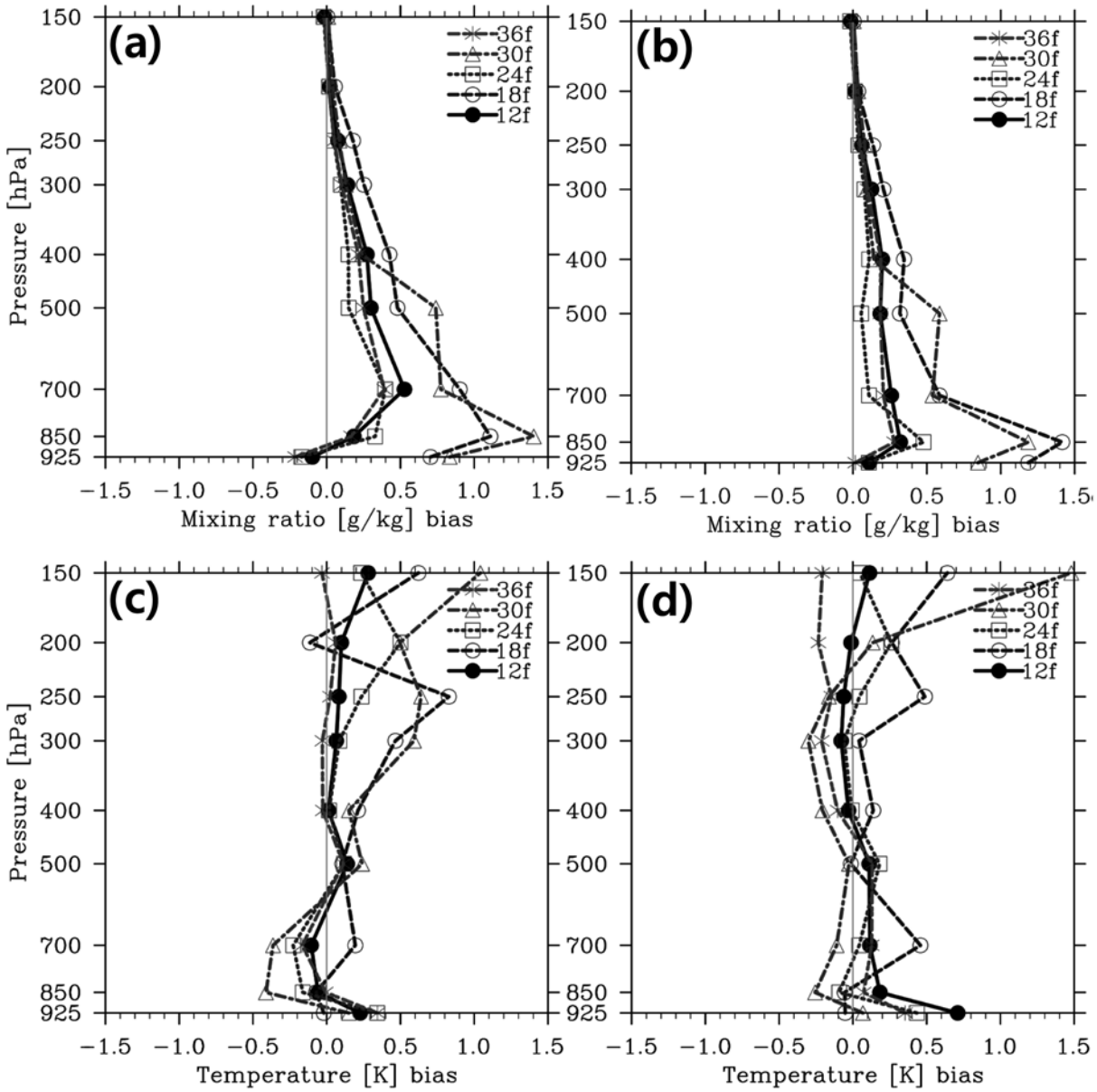

Fig. 6. Vertical distributions of mixing ratios and temperature biases between the radiosonde data and the experiments from 12 f (12 h forecast) to 36 f (36 h forecast) forecasts per 6 hour interval in domain 1: (a, c) CTRLD1 and (b, d) EXP1D1.

there is no noticeable difference in the temperature bias between the two experiments, although the differences are obvious in relation to the levels and forecast times.

Figure 7 shows the horizontal difference fields of the atmospheric variables derived from the FNL data and used in the experiments. CTRLD1 has large biases in the areas of large rainfall in the field of the geopotential height, subtropical high in the field of the temperature, and strong zonal wind in the field of

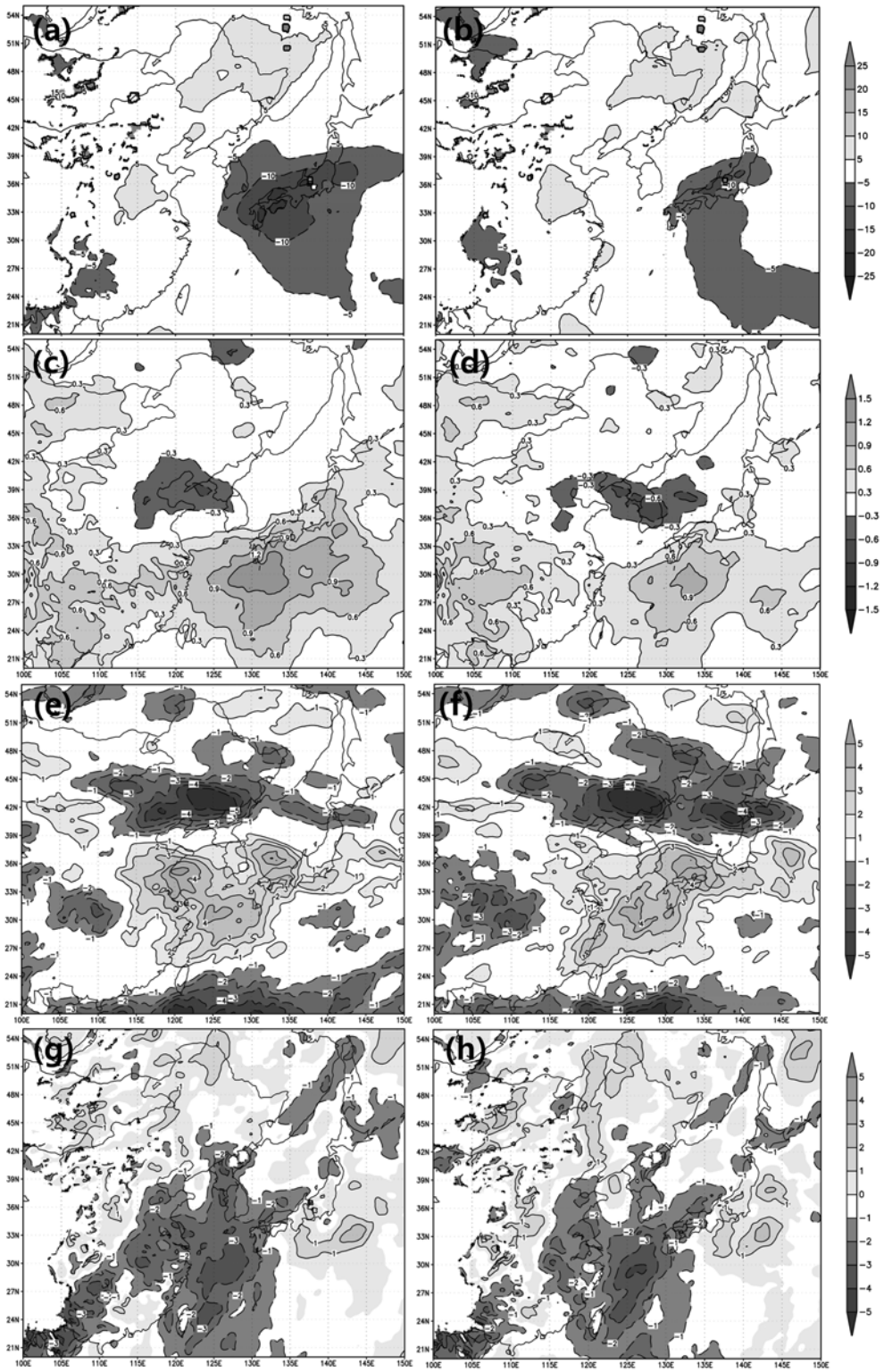

Fig. 7. Horizontal difference fields of (a, b) 850 hPa geopotential height, (c, d) 500 hPa temperature, (e, f) 300 hPa horizontal, and (g, h) 850 hPa meridional wind between the experiments and FNL data: (a, c, e, and g) CTRLD1, and (b, d, f, and h) EXP1D1.

the upper-level wind. EXP1D1 considerably reduces the biases in CTRLD1, except for the upper-level wind. In particular, the biases in CTRLD1 are also reduced by assimilating the GTS data in the area of the Korean Peninsula and nearby ocean.

The vertical distributions of the mixing ratio (a, b, c, and d) and temperature bias (e, f, g, and h) in domain 2 are shown in Fig. 8. EXP1D2 shows the improvements in the mixing ratio and temperature bias in CTRLD1, which are essentially similar to the improvements in domain 1. This implies that the improvement of the larger-scale features in domain 1 is important for forecast in the high-resolution nested model in which the GTS upper-air, wind profiler, and surface data are assimilated in the model domain. Surface data assimilation affects forecasts up to the 500 hPa level (EXP3D2). Weisman and Trapp (2003) showed that a storm environment with a significant low-level vertical wind shear probably influences the formation of a mesovortex. The horizontal distributions of 24 h accumulated rainfall during KEOP-2007 in domain 2, along with the TRMM data are shown in Fig. 9. According to the TRMM rainfall data (Fig. 9a), the areas to the east of China and to the south of Japan receive the largest amount of rainfall. In the Korean peninsula, weak rainfall is observed over the central and southwestern regions. CTRLD2 and EXP1D2 show that the rainfall amount in the rain band along the Changma front from East China to Japan is overestimated and that the rainfall amount in central Korea is underestimated compared to the observations. The rainfall predicted by EXP2D2 is comparable to the observed rainfall over central China, Japan, and the Korean peninsula; in particular, the predicted and observed values of the maximum rainfall in southern Japan and the second peak rainfall in the central region of the Korean Peninsula are comparable. EXP3D2 shows that less rainfall occurs over East China and Japan, and the rainfall region in the Korean Peninsula is widely extended, and the peak region is overestimated.

Figure 10 shows the difference fields for the 500 hPa geopotential height, 850 hPa wind vector, and 850 hPa water vapor mixing ratio for all CTRLD2 experiments in domain 2. In all experiments involving data assimilation, negative differences are observed in the mixing ratio over the seas to the south of Korea and Japan and in central China; in EXP2D2 and EXP3D2, positive differences are observed in the mixing ratio and geopotential height over the Yellow Sea. Positive differences in the southwesterly wind, which is part of an LLJ, are dominant over the western and southwestern parts of the Yellow Sea. In all the experiments involving data assimilation, negative differences in the westerly wind component contributed to less rainfall amount than that observed in CTRLD2. The geopotential height of EXP2D2 represents the positive difference in the northeastern part of Korea, implying that the inclusion of the upper-air data affected resulted in a strong Okhotsk high. In EXP3D3, the moisture and geopotential height increased only over South Korea. In particular, the data assimilation, including the upper-air data (EXP2D2), has a positive impact on the lower tropospheric fields such as moisture and wind at the 850 hPa level.

Tables 4 and 5 list the ETSs and BSs from the 1 h to 24 h rainfall forecasts in domain 3 for the rainfall for the entire period (ALL) and the heavy rainfall cases (HR). Seven heavy rainfall events were documented during the KEOP-2007 period. The ETS values for all of the threshold values are almost similar for all of the entire period rainfall experiments; the exception is the ETS values that tend to increase with data assimilation. However, the ETS values with data assimilation increase con-

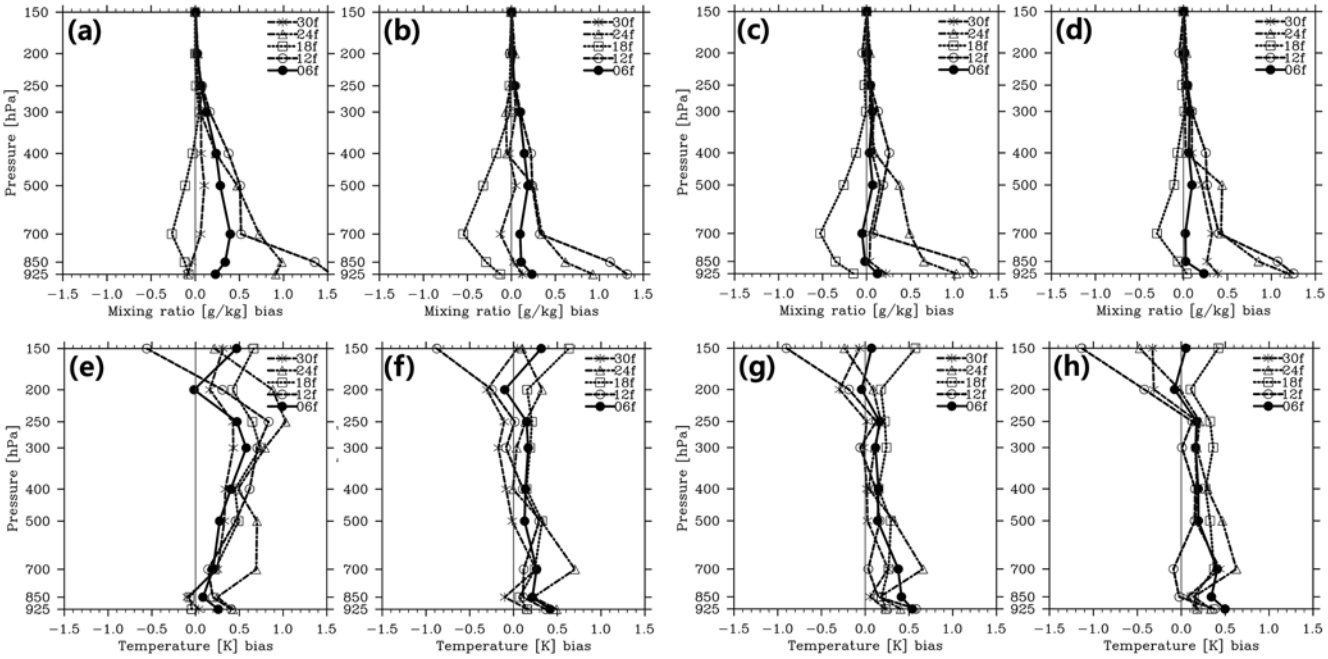

Fig. 8. Vertical distributions of mixing ratios (a, b, c, and d) and temperature biases (e, f, g, and h) in domain 2: (a, e) CTRLD2, (b, f) EXP1D2, (c, g) EXP2D2, and (d, h) EXP3D2.

siderably compared to those without data assimilation for the heavy rainfall cases; the increase is more pronounced for the combined assimilation of radar and AWS data. The BSs of the large threshold values (1.0 and 2.5 mm) reduce with radar and AWS data assimilation. The combined radar and AWS data assimilation contributed to improved rainfall forecasts obtained in this study.

In their research on the diurnal variation of rainfall over South Korea using data from the KMA surface station, Lim and Kwon (1998) analyzed the horizontal structure of the diurnal variation of precipitation over the South Korean peninsula for 17 years (1980-96). They found that the early morning or morning peak in precipitation in South Korea might be a global phenomenon with a minor variation in the time of occurrence. Misumi (1999) showed that the morning precipitation maximum over East Asia and the diurnal variation of the warm season precipitation are characterized by an afternoon maximum dominant for localized precipitation in Japan. Jung and Suh (2005) showed that the two

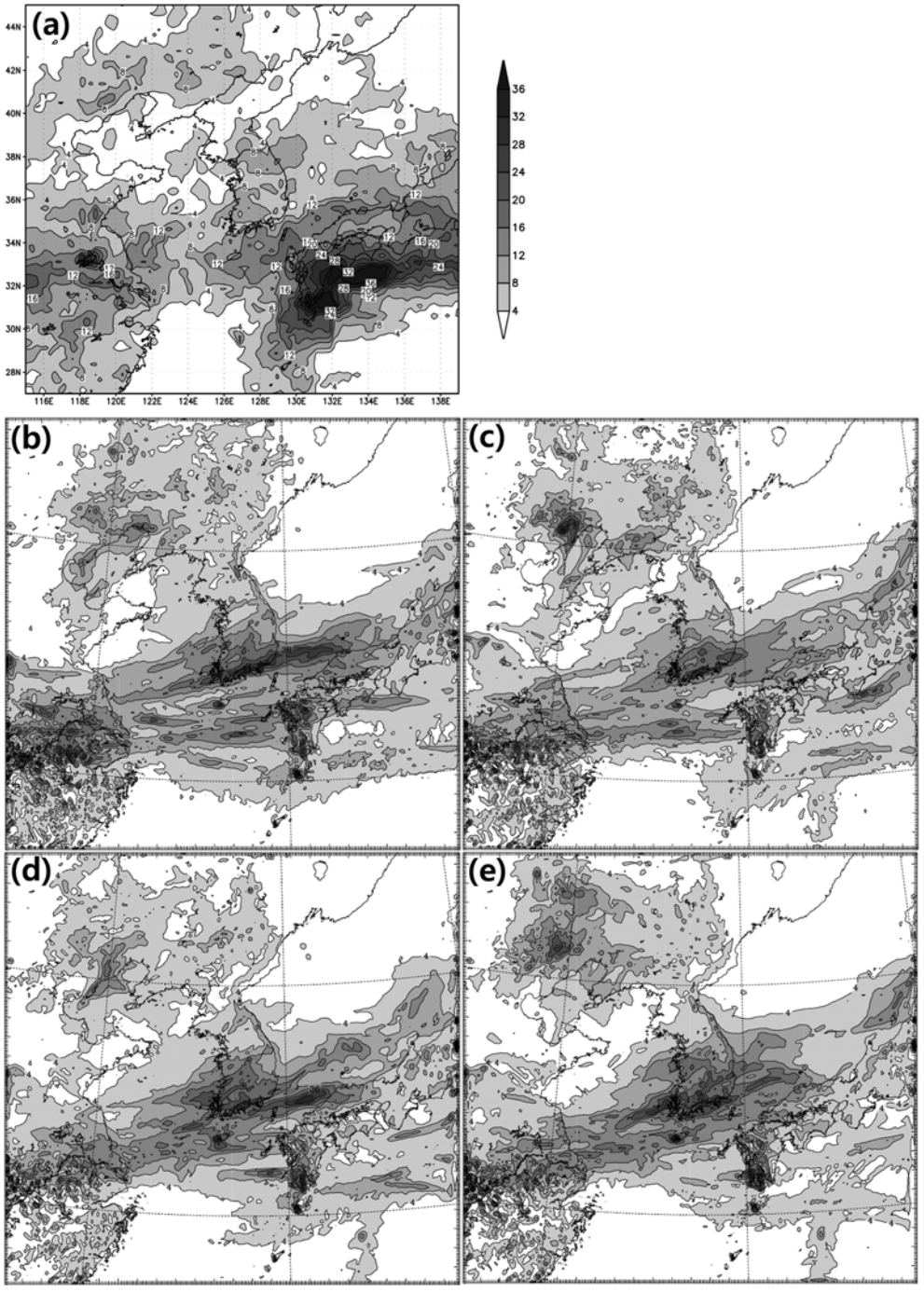

Fig. 9. Horizontal distributions of daily mean rainfall during KEOP-2007 in domain 2: (a) TRMM, (b) CTRLD2, (c) EXP1D2, (d) EXP2D2, and (e) EXP3D2.

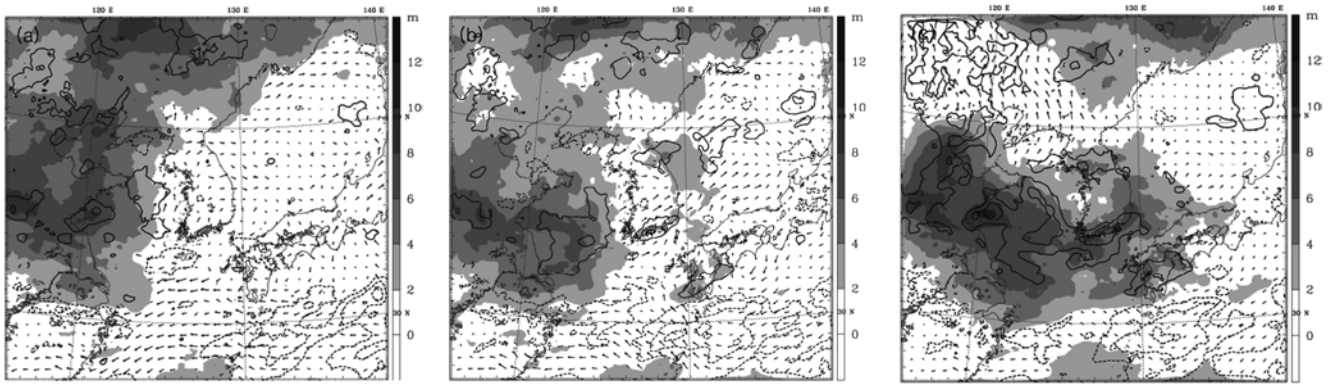

Fig. 10. Difference fields of synoptic environments ((500 hPa geopotential height [m]: shaded, 850 hPa wind vector and water vapor mixing ratio [0.5 g kg^{-1}]: positive (contour), negative (dashed)) at 24 h forecast from CTRLD2 in domain 2: (a) EXP1D2, (b) EXP2D2, and (c) EXP3D2.

Table 4. ETSs of rainfall from 1 h to 24 h rainfall forecasts in domain 3 for the entire period (ALL) and heavy rainfall (HR) cases.

Experiment	Threshold value	0.1 mm		1.0 mm		2.5 mm	
	Period	ALL	HR	ALL	HR	ALL	HR
CTRLD3		0.21	0.22	0.18	0.17	0.11	0.13
EXP1D3		0.22	0.28	0.19	0.25	0.12	0.16
EXP2D3		0.23	0.31	0.20	0.29	0.13	0.20
EXP3D3		0.22	0.34	0.20	0.31	0.13	0.22

Table 5. BSs of rainfall from 1 h to 24 h rainfall forecasts in domain 3 for the entire period (ALL) and heavy rainfall (HR) cases.

Experiment	Threshold value	0.1 mm		1.0 mm		2.5 mm	
	Period	ALL	HR	ALL	HR	ALL	HR
CTRLD3		1.31	0.81	0.81	0.58	0.77	0.62
EXP1D3		1.25	0.94	0.85	0.70	0.83	0.69
EXP2D3		1.20	0.96	0.93	0.73	0.90	0.73
EXP3D3		1.37	1.05	1.02	0.77	1.05	0.79

maxima of precipitation depend on the location; the afternoon maximum occurs over land, while the early morning maximum occurs over the west coastal region. In this study, the diurnal variation in rainfall over southern Korea is analyzed using model experiments in domains 2 and 3 (Fig. 11). The experiments with data assimilation show relatively better trends of the diurnal variation of rainfall. The maximum rainfall was observed at 1800 UTC during KEOP-2007 period. In domain 2, the peak time of hourly rainfall was captured, except for EXP2D2; while in domain 3, it was delayed by approximately 3 h and the rainfall amount was overestimated. The model predictability improves when the radar and AWS data are assimilated. The Changma season in Korea is mainly affected by synoptic-scale environment, so that data assimilation in domains 1 and 2 contribute to improved rainfall forecasting in domain 3.

Figure 12 shows the daily mean rainfall distribution in domain 3 with the TRMM data for the heavy rainfall cases. In all experiments, major maximum rainfall regions which occurred in the central and southern Korean Peninsula are predicted. The improvement of the mother domains directly affected the prediction of the rainfall distribution during the HR period in the nested domains. The radar assimilation not only helps predict localized rainfall in northwestern South Korea but also helps improve the predicted rainfall pattern in central South Korea. The AWS assimilation results in the Changma front being simulated further northward, so that the rainfall around the maximum rainfall region is overestimated, as seen in domain 2; further, rainfall is not predicted over the regions of Seoul and Kyunggi. Difference fields of the 700 hPa equivalent potential temperature (EPT) and wind vectors for the experiments with data assimilation from CTRLD3 in domain 3 are shown in Fig. 13. In all the experiments, the EPT differences increase over the southwestern and middle parts of the Korean Peninsula. In particular, the increased wind vector in the southwestern part of the model domain induces convergence over the maximum rainfall region and the increased EPT over the Kyunggi Bay increases the rainfall in EXP2D3. In EXP3D3, a greater increase in the EPT in the domain changes the south or southeasterly

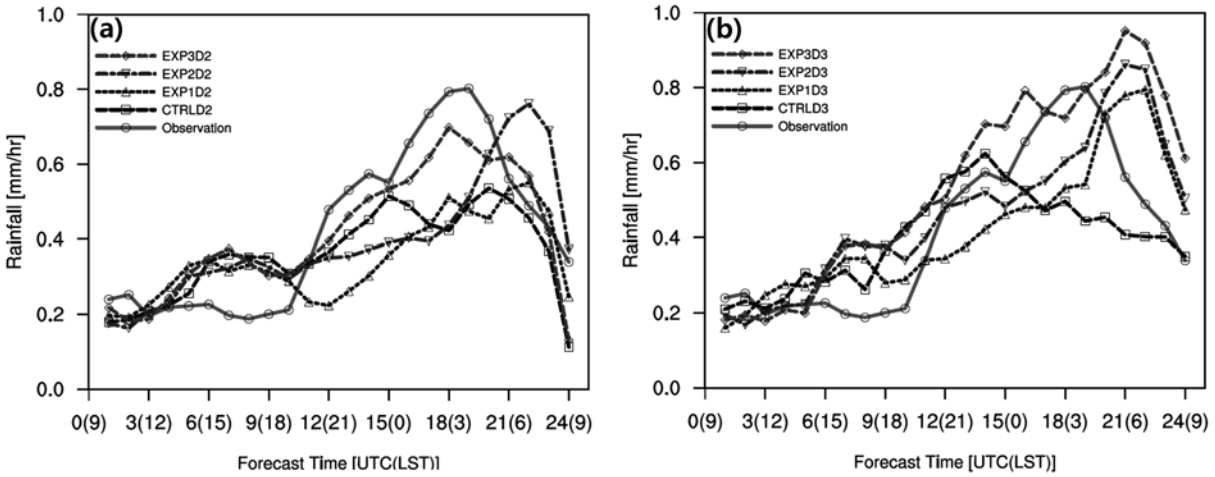

Fig. 11. Diurnal variation of rainfall over southern Korea analyzed using the model experiments in (a) domain 2, and (b) domain 3.

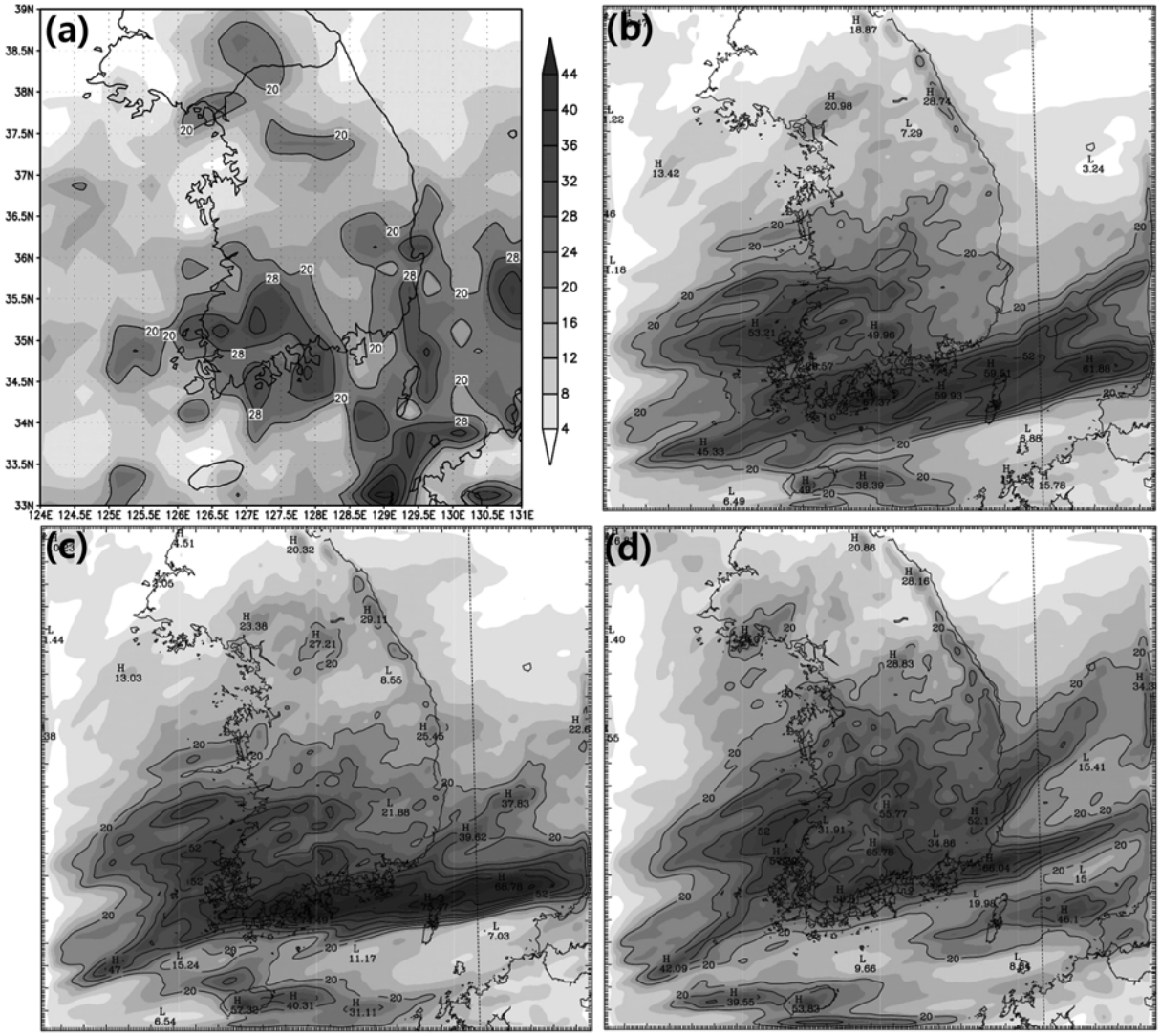

Fig. 12. Horizontal distribution of daily mean rainfall during the heavy rainfall cases in domain 3: (a) TRMM, (b) EXP1D3, (c) EXP2D3, and (d) EXP3D3.

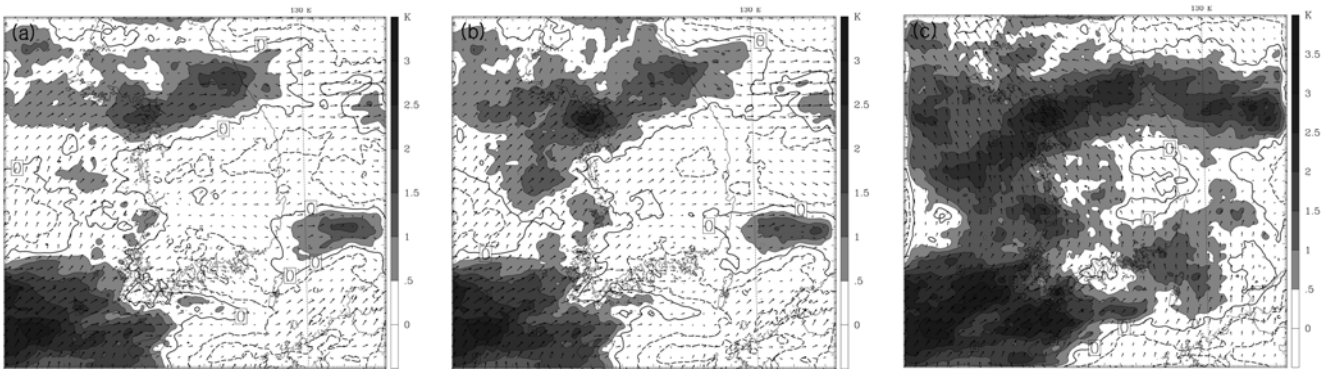

Fig. 13. Difference fields of 700 hPa equivalent potential temperature (solid lines are positive and dashed lines negative) and wind vector for the experiments with data assimilation from CTRLD3 in domain 3: (a) EXP1D3, (b) EXP2D3, and (c) EXP3D3.

wind at low levels, which affects the rain band and causes the maximum rainfall regions to move further northward.

5. Discussion and Conclusion

This study documents the rainfall validation of the real-time WRF forecasts over East Asia and the Korean Peninsula during the Changma season using the KEOP-2007 data. The data assimilation of RUC using the KEOP data is performed on the WRF-ARW model with three nested grids (horizontal resolutions: 27, 9, and 3 km). The forecast periods for the domains were 48, 36, and 24 h. The forecast rainfall amounts are verified against high-density rain gauge observations, GPCP, and TRMM. QPF using the forecast rainfall in domain 3 is estimated by calculating the ETS and BS scores.

During the Changma season, the monsoon rain band is observed to extend from south China to the south of Japan due to the strong development of the Okhotsk high. Heavy rainfall occurred when the NW Pacific subtropical high intensified and extended to the western Pacific warm pool, thereby affecting the variability of the summer monsoon rainfall patterns over South Korea. The GTS data assimilation in domain 1 results in better forecasts of the variables, which can be used as the improved forcing for the nested domains; hence, the Changma front is observed northward, and the moisture biases of the low and middle levels in domain 1 is reduced. Consequently, the synoptic environment affects the rainfall forecast in the Korean Peninsula in domains 2 and 3. The data assimilation in the mother domains is demonstrated to be necessary to provide an improved large-scale environment for the nested domains.

During KEOP period, the rainfall predictability of the model improved with data assimilation of GTS upper-air, wind profiler, AWS, and radar data in domains 2 and 3. Radar and AWS data assimilation improved the forecast rainfall in domain 3. The model predicts the observed diurnal variation in summer precipitation; peak time of rainfall is predicted to be at 3 and 4 LST over southern Korea. However, the rainfall is underestimated at 9-km horizontal resolution, and overestimated at 3-km resolution; at 3-km resolution, delayed peak of rainfall is simulated observed.

The results of this study demonstrated that data assimilation with WRF 3DVAR by utilizing various observations for KEOP-2007 improves the prediction of rainfall, especially for heavy rainfall, during the Changma season. However, further applications should be studied by using data from other observations, e.g., satellite observations. The experiment of horizontal and vertical retrieval-wind data assimilation using the radiance obtained from radar data (Park and Lee, 2009) is necessary because the wind values obtained from the WRF-3DVAR retrieval system depend on the background error of model wind. In addition to high horizontal resolution, observational and background error tuning in the model will be necessary because rainfall forecasts with assimilation of radar and AWS data is overestimated in this study. Huang *et al.* (2009) discussed that the 4DVAR algorithm can assimilate more observations than 3DVAR from high frequency fixed observing platforms, such as AWS networks, and Guo *et al.* (2008) shows that 4DVAR using radial velocity can be operated as a tool in the convective-scale weather research. Moreover, the comparison between 4DVAR and the Ensemble Kalman Filter (EnKF) will be in the context of the assimilation of real observations. The error in the forecast model and uncertainty in the specification of observational errors should be considered (Caya and Snyder, 2005). The KEOP data should be further studied with the 4DVAR and EnKF methods as well as sensitivity experiments of rainfall to the model physics implemented in the WRF model.

Acknowledgements. We thank the Mesoscale and Microscale Meteorology (MMM) division at the National Center for Atmospheric Research (NCAR) for collaborating with the WRF model. This study was supported by the Global Partnership Program of the Korea Foundation of International Cooperation for Science and Technology (KICOS). This study was also supported by the principal project "Development and application of technology for weather forecast (NIMR-2009-B-1)" of the National Institute of Meteorological Research of the Korea Meteorological Administration. Computing resources were supported by the Korea Institute of Science and Technology Information under "The Strategic Supercomputing Support Program."

REFERENCES

Anthes, R. A., Y.-H. Kuo, D. P. Baumhefner, R. M. Erico, and T.W. Bettge, 1985: Predictability of mesoscale atmospheric motions. *Adv. Geophys.*, **28B**, 159-202.

Barker, D. M., W. Huang, Y.-R. Guo, and A. Bourgeois, 2003: A three dimensional variational (3DVAR) data assimilation system for use with MM5. NCAR Tech. Note NCAR/TN-453STR, 68 pp.

_____, _____, _____, _____, and Q. Xiao, 2004: A three-dimensional variational (3DVAR) data assimilation system for MM5: Implementation and initial results. *Mon. Wea. Rev.*, **132**, 897-914.

Benjamin, S. G., and Coauthors, 2004a: An hourly assimilation/forecast cycle: The RUC. *Mon. Wea. Rev.*, **132**, 495-518.

_____, G. A. Grell, J. M. Brown, and T. G. Smirnova 2004b: Mesoscale weather prediction with the RUC hybrid isentropic-terrain-following coordinate model. *Mon. Wea. Rev.*, **132**, 473-494.

Caya, A., J. Sun. and C. Snyder, 2005: A comparison between the 4D-Var and the ensemble Kalman filter techniques for radar data assimilation. *Mon. Wea. Rev.*, **133**, 3081-3094.

Chen, S., J. E. Nachamkin, J. M. Schmidt, and C.-S. Liou, 2002: Quantitative precipitation forecast for the coupled ocean/atmosphere mesoscale prediction system (COAMPS). *19th Conf. on Weather Analysis and Forecasting/15th Conf. on Numerical Weather Prediction*, San Antonio, TX, Amer. Meteor. Soc., 7B.1. [Available online at http://ams.confex.com/ams/pdfpapers/47727.pdf.]

Chien, F.-C., Y. H. Kuo, and M.-J. Yang, 2002: Precipitation forecast of MM5 in the Taiwan area during the 1998 Mei-yu season. *Wea. Forecasting*, **17**, 739-754.

Clark, A. J., W. A. Gallus, and T. C. Chen, 2007: Comparison of the diurnal precipitation cycle in convective resolving and non-convection-resolving mesoscale models. *Mon. Wea. Rev.*, **35**, 3456-3473.

Colle, B., J. B. Olson, and J. S. Tongue, 2003a: Multiseason verification of the MM5. Part I: Comparison with the Eta model over the central and eastern United States and impact of MM5 resolution. *Wea. Forecasting*, **18**, 431-457.

_____, _____, and _____, 2003b: Multiseason verification of the MM5. Part II: Evaluation of high-resolution precipitation forecasts over the northeastern United States. *Wea. Forecasting*, **18**, 458–480.

Davis, C. A., K. W. Manning, R. E. Carbone, S. B. Trier, and J. D. Tuttle, 2003: Coherence of warm-season continental rainfall in numerical weather prediction models. *Mon. Wea. Rev.*, **131**, 2667–2679.

Grell, G. A., J. Dudhia, and D. R. Stauffer, 1994: A description of the fifth-generation Penn State-NCAR Mesoscale Model (MM5). NCAR Tech. Note NCAR/TN-398+STR, 122 pp.

Guo, Y.-R., J. Sun, E. Lim, X.-Y. Huang, X. Zhang, and S. Sugimoto, 2008: Assimilation of Doppler radar data with WRF 4DVAR for a convective case. *9th WRF Users' Workshop*, Boulder, Colorado. [Available online at http://www.mmm.ucar.edu/wrf-/users/workshops/WS2008/-abstracts/P5-06.pdf.]

Huang, X.-Y., and Coauthors, 2009a: Four-dimensional variational data assimilation for WRF: Formulation and preliminary results. *Mon. Wea. Rev.*, **137**, 299-314.

Jollie, I. T. and D. B. Stephenson, 2003: *Forecast Verification: A Practitioner's Guide in Atmospheric Science*. Wiley and Sons Ltd., 254 pp.

Joly, A., and Coauthors, 1999: Overview of the field phase of the Front and Atlantic Storm-Track Experiment (FASTEX) project. *Quart. J. Roy. Meteor. Soc.*, **125**, 3131-3163.

Jung, J.-H., and M.-S. Suh, 2005: Characteristics and types of the diurnal variation of hourly precipitation during rainy season over South Korea. *J. Korean Meteor. Soc.*, **41**, 533-546. (in Korean with English abstract)

Kim, H.-H., and S.-K. Park, 2008: Current Status of Intensive Observing Period and Development Direction. *Atmosphere*, **18**, 147-158. (in Korean with English abstract)

Kim. H.-W., and D.-K. Lee, 2006: An Observational Study of Mesoscale Convective Systems with Heavy Rainfall over the Korean Peninsula. *Wea. Forecasting*, **21**, 125-148.

Kuo, Y.-H., and G. T.-J. Chen, 1990: The Taiwan Area Mesoscale Experiments: An overview. *Bull. Amer. Meteor. Soc.*, **71**, 488-503.

Langland, R. H., and Coauthors, 1999: The North Pacific Experiment (NORPEX-98): Targeted observations for improved North American weather forecasts. *Bull. Amer. Meteor. Soc.*, **80**, 1364-1384.

Lee, D.-K., S.-Y. Hong, and S.-O. Hwang. 1991: Evolution of mesoscale feature associated with two extremely heavy rainfall events occurred over the Korean Peninsula. *Proc. Int. Conf. on Mesoscale Meteorology and TAMEX*, Taipei, Taiwan, Taiwan Meteor. Soc. and Amer. meteor. Soc., 284-288.

_____, H.-R. Kim, and S.-Y. Hong, 1998: Heavy rainfall over Korea during 1980-1990. *Korean J. Atmos. Sci.*, **1**, 523-547. (in Korean with English abstract)

_____, J.-W. Kim, D.-Y. Eom, S.-J. Choi, and J.-H. Ha, 2008a: WRF Real-Time Operation at JHWC-GPP. *2nd East Asia WRF Workshop and Tutorial*, Seoul, Korea. [Available online at http://jhwc.snu.ac.kr/wrf2008/workshop_ppt/2-1.pdf.]

_____, J.-G. Park, and J.-W. Kim, 2008b: Heavy Rainfall Events Lasting 18 Days from July 31 to August 17, 1998, over Korea. *J. Meteor. Soc. Japan*, **86**, 313-333.

_____, J.-W. Kim, D.-Y. Eom, S.-J. Choi, and J.-H. Ha, 2009: Data assimilation of the JHWC real-time WRF system. *3rd East Asia WRF Workshop and Tutorial*, Seoul, Korea. [Available online at http://jhwc.snu.ac.kr/wrf2009/presentation /1/1-5.ppt]

Lee, W.-C., and Ben J.-D. Jou, 2008: An overview of SoWMEX/TiMREX operation. *1st SoWMEX/TiMREX Science Workshop*, Taipei, Taiwan. [Available online at http://sowmex.cwb.gov.tw/2008/showppt.php?SessW=17_DongKyouLee&-pptDate=20081106.]

Lim, G.-H., and H.-J. Kwon, 1998: Diurnal variation of precipitation over South Korea and its implication. *J. Korean Meteor. Soc.*, **34**, 222-237. (in Korean with English abstract)

Misumi, Y., 1999: Diumal variations of precipitation grouped into cloud categories around Japanese archipelago in the warm season. *J. Meteor. Soc. Japan*, **77**, 615-635.

Ninomiya, K., and C. Kobayashi, 1998: Precipitation and moisture balance of the Asian summer monsoon in 1991. Part I: Precipitation and major circulation systems. *J. Meteor. Soc. Japan*, **76**, 855-877.

Park, S.-G., and D.-K. Lee, 2009: Retrieval of high-resolution wind fields over southern Korean Peninsula using doppler weather radar network. *Wea. Forecasting*, **24**, 87-103.

Skamarock, W. C., J.B. Klemp, J. Dudhia, D. O. Gill, D. M. Barker, W. Wang, and J. G. Powers, 2005: A description of the Advanced Research WRF Version 2. NCAR Tech. Note 468STR, 88 pp.

Sun, J., and T.-Y. Lee, 2002: A numerical study of an intense quasi-stationary convection band over the Korean Peninsula. *J. Meteor. Soc. Japan*, **80**, 1221-1245.

Warner, T. T., R. A. Peterson, and R. E. Treadon, 1997: A tutorial on lateral boundary conditions as a basic and potentially serious limitation to regional numerical weather prediction. *Bull. Amer. Meteor. Soc.*, **78**, 2599-2617.

Weckwerth, T. M., D. B. Parsons, S. E. Koch, J. A. Moore, M. A. Lemone, B. B. Demoz, C. Flamant, B. Geerts, J. Wang, and W. F. Feltz, 2004: An overview of the international H2o project (IHOP_2002) and some preliminary highlights. *Bull. Amer. Meteor. Soc.*, **85**, 253-277.

Weisman, M. L., and R. J. Trapp, 2003: Lowlevel mesovortices within squall-lines and bow echoes: Part I. Overview and dependence on environmental shear. *Mon. Wea. Rev.*, **131**, 2779-2803.